Electron Transfer in Tetrahemic Cytochromes c_3: Spectroelectrochemical Evidence for a Conformational Change Triggered by Heme IV Reduction†

Irina Kazanskaya,‡,§ Doris Lexa,|| Mireille Bruschi,|| and Geneviève Chottard*,‡

Chimie des Métaux de Transition, Université Pierre et Marie Curie, Case 42, 75252 Paris Cedex 05, France, and CNRS, BIP, Chemin Joseph Aiguier, 13402 Marseille Cedex 20, France

Received April 8, 1996; Revised Manuscript Received June 24, 1996⊗

ABSTRACT: Electron transfer in tetrahemic cytochromes c_3 from *Desulfovibrio vulgaris* Hildenborough (D.v.H.) and *Desulfovibrio desulfuricans* Norway (D.d.N.) strains has been investigated by thin layer spectroelectrochemistry with visible absorption, CD, and resonance Raman (RR) monitoring. The observed splitting of the isosbestic point in the Soret absorption band indicates that the electron transfer from the $(Fe^{III})_4$ state to the $(Fe^{II})_4$ state proceeds via an intermediate species, which corresponds to 25 and 50% reduction for the D.v.H. cyt. c_3 and the D.d.N. cyt.c_3, respectively. For the latter, a specific CD signal is observed at half-reduction. RR monitoring of the redox process does not reveal multiple splitting of the high-frequency RR bands, at variance with previously published results on the enzymatic reduction of cyt.c_3 from *Desulfovibrio vulgaris* Miyazaki, a cytochrome highly homologous to D.v.H. cyt.c_3 [Verma, A. L., Kimura, A., Nakamura, A., Yagi, T., Inoguchi, H., & Kitagawa, T. (1988) *J. Am. Chem. Soc. 110*, 6617−6623]. The low-frequency RR spectra of the intermediate species differ significantly from the ones calculated from a linear combination of the all-ferric and all-ferrous states, for the same reduction ratio. Frequency shifts of the bending modes of the cysteine and propionate heme substituents are observed, as well as changes specific to each cytochrome; most notable is the activation of two torsional modes in the case of D.d.N. cyt.c_3. Comparison of the results obtained for the two cytochromes leads to the conclusion that reduction of heme IV triggers the observed conformational change. This conclusion is supported by the spectroelectrochemical investigation of the mutant D.v.H. cyt.c_3 H25M, in which the sixth ligand of heme III, histidine, is replaced by a methionine.

Cytochromes c_3 are a class of multiheme cytochromes found in sulfate-reducing bacteria that are supposed to function as electron carriers for hydrogenase (Postgate, 1984; Le Gall & Fauque, 1988). Four of these proteins have been extensively studied: cytochromes c_3 Hildenborough and Miyazaki both originating from the *Desulfovibrio vulgaris* (D.v.) species (86% homologous), cytochrome c_3 Norway from *Desulfovibrio desulfuricans* (D.d.), and cytochrome c_3 Gigas from *Desulfovibrio gigas* (D.g.). They contain four bis-histidine-liganded hemes, covalently bound by two thioether linkages to a single polypeptide chain (M_r of *ca.* 14 000). Their three-dimensional structures were solved first for D.d.N. cyt.c_3 (Pierrot et al., 1982) and then for D.v.M. (Higuchi et al., 1984) and D.v.H. (Morimoto et al., 1991) cyt.c_3. Despite the limited sequence homology between D.d.N. cyt.c_3 and the D.v. cyt.c_3, the three-dimensionnal structures of these cytochromes are very similar; they are built of well-conserved structural domains (for example, the heme binding domains) linked by outward pointing loops of variable lengths (Morais et al., 1995).

Cytochromes c_3 exhibit very negative redox potentials of ca. −300 mV vs NHE: the four hemes have different potentials, but their values are so close that voltammetric measurements (to which cyt.c_3 responds readily) display only one or two waves, from which the four values have to be extracted by deconvolution procedures (Sokol et al., 1980; Bianco & Haladjian, 1981; Moreno et al., 1989). Various attempts, mainly based on EPR and NMR spectroscopies, which offer the possibility of discriminating among the four hemes, have been made in order to assign a redox potential to specific hemes. From an EPR study of a single crystal of D.d.N. cyt.c_3, Guigliarelli et al. (1990) have proposed the following order for the redox potentials (hemes numbered according to the sequence order of the binding cysteinyl residues), HIII > HIV > HI > HII, which was confirmed recently by an NMR study of Coutinho et al. (1993). For D.v.M. cyt.c_3, an NMR study by Fan et al. (1990) has led to the following order, HIV > HI > HIII > HII, whereas Salgueiro et al. (1992) have proposed HIV > HI > HII > HIII for the homologous D.v.H. cyt.c_3.

Kinetic studies of the electron transfer have been undertaken under various conditions, using chemical reductants (Tabushi et al., 1983; Capellière-Blandin et al., 1986; Catarino et al., 1991) or enzymatic reductants (Yagi, 1984; Capellière-Blandin et al., 1986). Biphasic kinetics were observed in all cases, except when the redox partner was ferredoxin (Capellière-Blandin et al., 1986). In the reduction by sodium dithionite (Tabushi et al., 1983; Capellière-

† This work received financial support from a CNRS grant (IMABIO program). I.K. was supported by a Graduate Fellowship from the French government.

‡ Universite Pierre et Marie Curie.

§ Present address: Kurnakov Institute of General and Inorganic Chemistry, 31a Leninski Prospekt, Moscow, Russia.

|| CNRS.

⊗ Abstract published in *Advance ACS Abstracts,* September 1, 1996.

[1] Abbreviations: cyt.c_3, cytochrome c_3; D.v.H., *Desulfovibrio vulgaris* Hildenborough; D.d.N., *Desulfovibrio desulfuricans* Norway, recently reclassified as *Desulfomicrobium baculatum* Norway 4 (Devereux et al., 1990); D.v.M., *Desulfovibrio vulgaris* Miyazaki; HI−IV, hemes numbered according to the sequence order of the binding cysteinyl residues; RR, resonance Raman.

S0006-2960(96)00842-2 CCC: $12.00

Blandin et al., 1986; Catarino et al., 1991), the relative importance of the fast phase seems to depend on the cyt.c_3 under consideration.

Monitoring of the reduction of cyt.c_3 by Soret absorption (Tabushi et al., 1983; Yagi, 1984), CD (Tabushi et al., 1983), and EPR (Guigliarelli et al., 1990) has led to the conclusion that an intermediate is involved in the process. Recent results obtained by FTIR spectroelectrochemistry have also shown the existence of an intermediate, with distinctive vibrational frequencies, in the case of D.d.N. cyt.c_3 and Gigas cyt.c_3 (Schlereth et al., 1993).

In the present work, we investigate the electron transfer in two different cytochromes, *D. vulgaris* Hildenborough (hereafter D.v.H.) and *D. desulfuricans* Norway (hereafter D.d.N.), by thin layer spectroelectrochemistry, with visible absorption, circular dichroism (CD), and resonance Raman (RR) monitoring. Soret absorption monitoring shows that an intermediate is involved in the process, in agreement with previously published results on D.d.N. cyt.c_3 (Schlereth et al., 1993), D.g.G. cyt.c_3 (Schlereth et al., 1993), and D.v.M, cyt.c_3 (Tabushi et al., 1983; Yagi, 1984). CD and RR spectroelectrochemical studies allow further characterization of this intermediate state. A comparative visible spectroelectrochemical study of the electron transfer in the D.v.H. cyt.c_3 mutant H25M, in which the replacement of the sixth ligand of heme III by a methionine leads to an increase of the corresponding redox potential, is reported. Taken altogether, our results suggest that the oxidoreduction of heme IV is the trigger of the conformational change that we observe for these cytochromes, independent of the position of its redox potential in the sequence order of the four heme potentials.

MATERIALS AND METHODS

D.d.N. (NCIB 8310) and D.v.H. (NCIB 8303) cytochromes c_3 were purified according to published methods (Bruschi et al., 1977; Le Gall et al., 1965). Tris-HCl and cacodylate buffers at 50 mM concentrations were used in the pH 7.2−9.2 and 5.5−7 range, respectively.

The H25M mutant of D.v.H. cyt.c_3 was prepared as previously described (Dolla et al., 1994).

The electrochemical cell was derived from the cell described by Lexa et al. (1977); it was based on a 0.05 cm absorption cell modified so as to offer a large neck providing space to accommodate the electrodes and the Ar gas inlet. The working electrode was a gold grid positioned in the optical path and used without any surface modification; the counter electrode was a Pt wire semi-isolated from the solution under study by porous glass, and the reference electrode was an Ag/AgCl electrode. Both electrodes were positioned in the upper part of the cell. The potential of our reference electrode in the buffer measured vs SCE was +35 mV. The cell and solutions (30−50 mM in cyt.c_3) were fully degassed under Ar before experiments.

The UV−visible absorption measurements were carried out either on a Cary 219 spectrometer or on a Shimadzu 2001 UV PC spectrometer at room temperature. The applied potential was maintained for the time required to get superimposition of two spectra, recorded at an interval of a few minutes (typical total time of 30 min), and then incremented by 20−30 mV until another equilibrium was obtained. For each potential, the amount of reduced species was determined from the absorbance at 553 nm, by calculating the ratio $(A - A_0)/(A_r - A_0)$, where A_0 and A_r are the absorbances at 553 nm of the fully oxidized and fully reduced species, respectively. Following each reduction experiment, complete reoxidation was achieved in order to check that the final spectrum was identical to the starting spectrum. For oxidation experiments, the solution was first fully reduced at −550 mV and then reoxidized step by step.

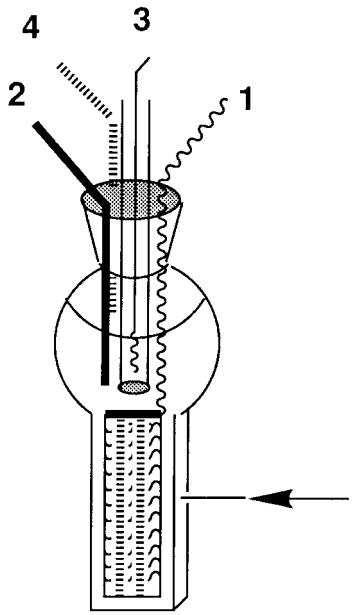

FIGURE 1: Raman spectroelectrochemical cell: (1) bare gold grid used as the working electrode, (2) Ag/Ag^+ reference electrode, (3) Pt thread used as the counter electrode, and (4) argon inlet. The arrow indicates the incident laser beam.

The CD measurements were run on a JY MarkIV Dichrograph. Either the procedure previously described was used, or, in some instances, the solution under study was first brought to the desired reduction stage by visible absorption monitoring and then examined by CD.

The RR spectra were obtained on a JY U1000 double monochromator. For Soret excitation, the 413.1 nm line of a Coherent Kr^+ laser with 8−10 mW of power was used; for $\alpha\beta$ excitation, the 514.5 nm line of a Coherent Ar^+ laser was used with 50−80 mW of power. An AsGa photomultiplier was used with photon-counting electronics. The spectral slit width was 4 cm^{-1} at 514.5 nm and 6 cm^{-1} at 413.1 nm. The electrochemical cell designed for RR spectroscopy (Figure 1) was made of a quartz fluorescence cell with a 1 mm optical path. This cell fits into the visible spectrometer so that the achieved reduction stage of the solution could be checked before and after the recording of the Raman spectrum. This was necessary in order to correctly characterize the intermediate species. cyt.c_3 concentrations between 50 and 100 μM were used, depending on the excitation wavelength.

RESULTS

Visible Absorption Spectroelectrochemistry

The absorption spectra of D.v.H. cyt.c_3 obtained after equilibration at increasingly negative potentials display five isosbestic points, but strikingly, in the Soret region, the sixth crossing area encompasses two distinct points A and B (Figure 2). Point A is located at 414.4 nm and corresponds

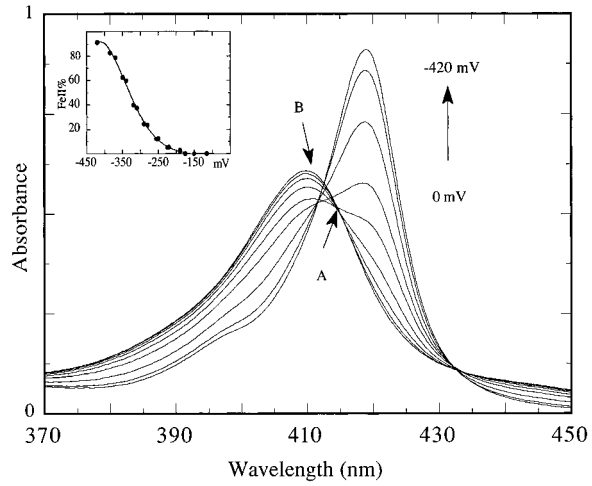

FIGURE 2: Absorption spectra of D.v.H. cyt.c_3 in the Soret band (Tris-HCl buffer, 50 mM, pH 7.5), at increasingly negative potentials (reduction ratios are indicated in parentheses) from 0 mV $(Fe^{III})_4$ to −420 mV $(Fe^{II})_4$: 0 (0%), −190 mV (2%), −225 mV (5%), −255 mV (12%), −290 mV (24%), −320 mV (39%), −350 mV (63%), −385 mV (83%), −420 mV (91%). (Inset) Titration plot.

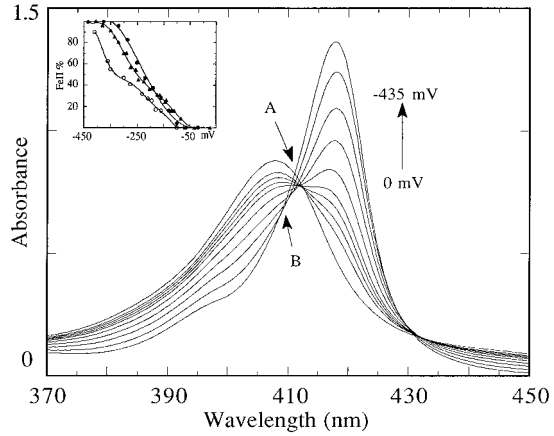

FIGURE 3: Absorption spectra of D.d.N. cyt.c_3 in the Soret band (Tris-HCl buffer, 50 mM, pH 7.5), at increasingly negative potentials (reduction ratios are indicated in parentheses) from 0 mV $(Fe^{III})_4$ to −435 mV $(Fe^{II})_4$: 0 (0%), −120 mV (16%), −145 mV (24%), −175 mV (31%), −205 mV (36%), −245 mV (45%), −275 mV (57%), −300 mV (70%), −335 mV (86%), and −435 mV (100%). (Inset) Titration plot: (▲) pH 7.5, (○) pH 9.2, and (●) ionic strength of 0.5 M.

to the first step of the reduction, while point B is located at 412 nm and corresponds to the end of the reduction. The switch between A and B occurs at 25% reduction. Careful examination of the other isosbestic points suggests that some of them may be considered as very close doublets with wavelength separation hardly larger than the limit of accuracy of the measurements. The same results are obtained for the reoxidation process.

Analogous results have been obtained for D.d.N. cyt.c_3 (Figure 3); points A and B are located at 412.6 and 410.8 nm, respectively, and the switch between A and B occurs at 50% reduction.

The occurrence of isosbestic points in the course of a spectrophotometric titration means that only two species are in equilibrium. Therefore, these results suggest that the overall redox process occurs via an intermediate oxidation state corresponding to the following scheme:

$$(Fe^{III})_4 \rightleftharpoons (Fe^{III})_3(Fe^{II}) \rightleftharpoons (Fe^{II})_4 \quad \text{for D.v.H. cyt.}c_3$$

$$(Fe^{III})_4 \rightleftharpoons (Fe^{III})_2(Fe^{II})_2 \rightleftharpoons (Fe^{II})_4 \quad \text{for D.d.N. cyt.}c_3$$

From these data, plots of the reduction ratio vs applied potential have been drawn. For D.v.H. cyt.c_3, the plot (Figure 2) is a sigmoid curve giving a mean value of the potential equal to −330 ± 5 mV at pH 7.5. For D.d.N. cyt.c_3, the titration curve, which agrees with the previously published ones (Schlereth et al., 1993), displays a plateau, showing that the first reduction potential is clearly higher than the others (Figure 3) and therefore can be determined straightforwardly; $(E_{1/2})_1 = -120$ mV, in agreement with Moreno et al. (1991).

The influence of pH has been studied in the pH 5.8−9.2 range. No significant variations of the isosbestic points have been observed, whereas the potential values are modified, at the lower or higher ends; a 25 mV upshift is observed at low pH for D.v.H. cyt.c_3, and for D.d.N. cyt.c_3, the titration curve is displaced toward lower potential values [$(E_{1/2})_1 = -160$ mV] at pH 9.2 and a second plateau is seen at midreduction.

The influence of ionic strength has been investigated also (experiments run in the presence of 0.5 M NaCl); no change has been observed for D.v.H. cyt.c_3, whereas for D.d.N. cyt.c_3, the second part of the curve is upshifted (+40 mV) while the first plateau remains unchanged.

In the course of these experiments, an influence of the protein concentration was noticed. At 100 mM, the reversibility of the process becomes poorer; the reduction steps require potentials ca. 50 mV lower and the oxidation steps potentials ca. 50 mV higher than at 50 mM. A similar influence of the protein concentration was already mentioned in the case of direct voltammetry of horse heart cyt.c (Hagen, 1989); reversibility was lost at 300−350 mM, and the potential was lowered at 1.3 mM.

Characterization of the Intermediate State

UV−visible, CD, and RR spectra have been obtained for the intermediate states revealed by the UV−visible spectroelectrochemical study and compared to the calculated spectra, for the same reduction ratio x, S_x, obtained by a linear combination of the spectra of the all-ferric (S_{ox}) and of the all-ferrous (S_{red}) species; $S_x = (100 - x)S_{ox} + xS_{red}$.

UV−Visible Difference Spectroscopy. The difference spectra of cyt.c_3 reduced at potential E minus oxidized cyt.c_3, E being the potential at which 25 and 50% reduction is achieved, are shown on Figure 4. From the comparison with the calculated spectra, $S_x - S_{ox}$, it comes out clearly that, for D.v.H. cyt.c_3 in the intermediate state (Figure 4a), the Fe(II) component has red-shifted bands (+1 nm in the Soret, +2 nm in the α band), the corresponding missing high potential Fe(III) component appearing as a negative red-shifted band in the Soret (+4 nm). For D.d.N. cyt.c_3 in the intermediate state (Figure 4b), the Fe(II) component is not displaced, while the corresponding Fe(III) component is red-shifted (+2 nm). These results suggest that the λ_{max} and/or the intensity of the absorption components in the intermediate states is different from those of the all-ferric and all-ferrous states, this being consistent with the presence of nonunique isosbestic points, in the course of the spectrophotometric titration of the redox reaction.

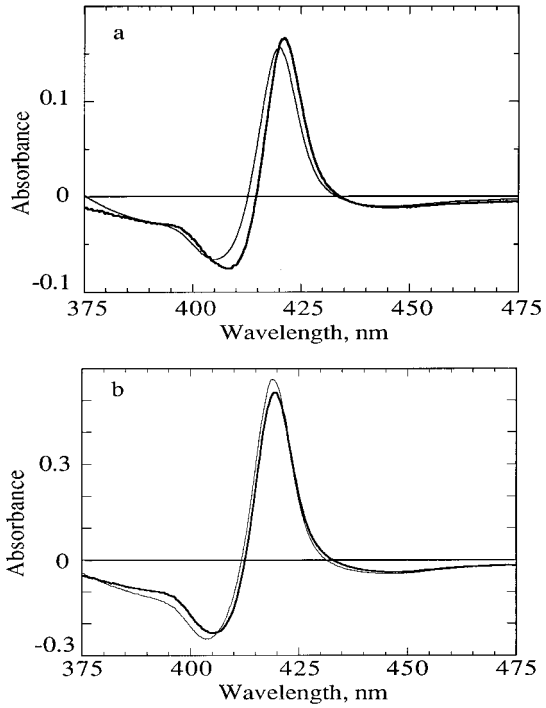

FIGURE 4: Soret differential absorption spectra (spectrum at potential E − spectrum at potential 0, E = potential to achieve 25 or 50% reduction). (a) D.v.H. cyt.c_3: (dark line) experimental and (light line) calculated, for 25% reduction. (b) D.d.N. cyt.c_3: (dark line) experimental and (light line) calculated, for 50% reduction.

Table 1: Wavelength (λ_{max} in nm) and Intensity ($\Delta\epsilon$ in M^{-1} cm^{-1}) of the Soret CD Bands

cyt.c_3	$(Fe^{III})_4$, λ_{max} ($\Delta\epsilon$)	$(Fe^{II})_4$, λ_{max} ($\Delta\epsilon$)	intermediate experimental	intermediate calculated
D.v.H.	410.5 (+380)	420 (+800)	410 (+220)	408 (+230)
	423 (−33)	426 (−200)	416 (+160)	419 (+120)
				427 (−70)
D.v.N.	406 (+360)	418 (+450)	412 (+295)	409 (+260)
	421 (−20)	425 (−70)	422 (−130)	418 (+230)
				425 (−45)

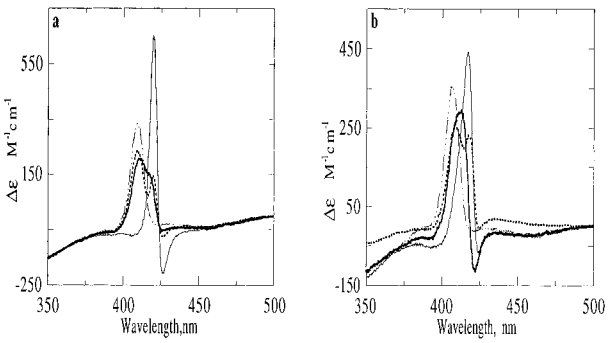

FIGURE 5: Soret CD spectra. (a) D.v.H. cyt.c_3: (−···−) $(Fe^{III})_4$, (light line) $(Fe^{II})_4$, and (dark line) $(Fe^{III})_3(Fe^{II})$ experimental; (···) $(Fe^{III})_3(Fe^{II})$ calculated, (b) D.d.N. cyt.c_3: (−···−) $(Fe^{III})_4$; (light line) $(Fe^{II})_4$, (dark line) $(Fe^{III})_2(Fe^{II})_2$ experimental; (···) $(Fe^{III})_2$-$(Fe^{II})_2$ calculated.

Circular Dichroism. The Soret CD data of both cytochromes c_3 are given in Table 1. For the ferric species, the CD signal consists of a strong positive band accompanied by a shallow negative trough, whereas the ferrous species exhibit an excitonic, though non conservative, signal (Figure 5). The CD signal of D.v.H. cyt.c_3 in the intermediate state (Figure 5a) is composed of a positive band at 410 nm with a shoulder at 416 nm; when that spectrum is compared to the calculated spectrum, it appears clearly that the ferrous heme contribution has no excitonic character. The CD signal of D.d.N. cyt.c_3 in the intermediate state (Figure 5b) is composed of a strong positive band at 412 nm and a negative band at 422 nm; thus, it offers no resemblance with the calculated spectrum.

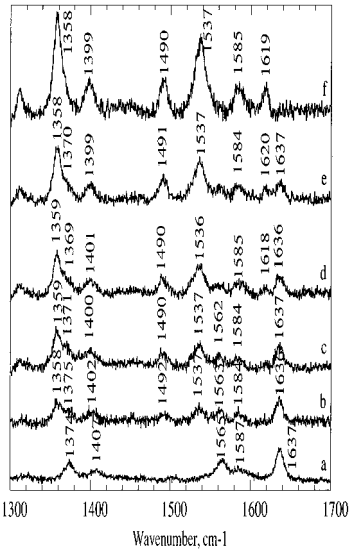

FIGURE 6: High-frequency RR spectra of D.v.H. cyt.c_3, recorded in the course of a progressive electrochemical reduction (excitation, 514.5 nm, 80 mW): (a) no potential, $(Fe^{III})_4$; (b) −290 mV, 25% Fe(II); (c) −315 mV, 38% Fe(II); (d) −345 mV, 62% Fe(II); (e) −375 mV, 80% Fe(II); and (f) −500 mV, $(Fe^{II})_4$.

Resonance Raman Spectra. The RR spectra of both cytochromes c_3 at various stages of reduction have been recorded with Soret (413.1 nm) and $\alpha\beta$ excitation (514.5 nm). Two frequency regions have been explored: the 1300−1700 cm^{-1} region, which displays the heme-stretching vibrations that are used as oxidation and spin state marker frequencies, and the 200−800 cm^{-1} region, which displays the tetrapyrrole deformation and the ring substituent deformation modes. Due to symmetry consideration, the high-frequency spectrum is richer when obtained with $\alpha\beta$ excitation, as it contains all symmetry type vibrations, whereas with Soret excitation, the spectrum is restricted to totally symmetric modes; therefore, we present here the spectra with 514.5 nm excitation. In the low-frequency region, due to the larger cross section of Soret excitation, we present the spectra obtained with 413.1 nm excitation.

In the high-frequency region, the spectra of both cytochromes are almost identical for the $(Fe^{III})_4$ and the $(Fe^{II})_4$ states and are in good agreement with the previously published data on cyt.c_3 Miyazaki (Kitagawa et al., 1975, 1977). In Figure 6 are shown the spectra recorded in the course of the electrochemical reduction of D.v.H. cyt.c_3; contrary to the results reported for the progressive reduction of D.v.M. cyt.c_3 by hydrogen in the presence of hydrogenase (Verma et al., 1988), no multiple splittings of the main Raman bands are observed. The spectrum of D.d.N. cyt.c_3, in the intermediate state (half-reduction), is shown in Figure 7; all the bands correspond to either a Fe(II) or Fe(III) component, as demonstrated by the very good agreement, in both frequencies and relative intensities, between the experimental spectrum and the spectrum calculated from the all-ferric and all-ferrous states, for half-reduction.

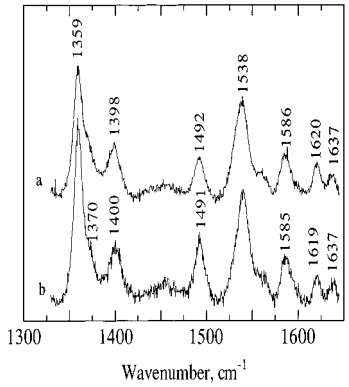

FIGURE 7: High-frequency RR spectra of D.d.N. cyt.c_3, in the intermediate state (excitation, 413.1 nm, 10 mW): (a) experimental and (b) calculated.

Table 2: RR Frequencies of Cytochromes c_3 in the 750−150 cm^{-1} Range[a]

	D.d.N				D.v.H			
mode	$(Fe^{III})_4$	$(Fe^{II})_4$	inter exp	inter calc	$(Fe^{III})_4$	$(Fe^{II})_4$	inter exp	inter calc
ν_{15}	750	749				748	751	
γ_5		734	732	734				
γ_{11}	713 sh	715 sh	713	718 sh	717	720	718	717
ν_7	702 sh				696		699 sh	
ν C_aS	687				685	684	684	685
ν C_aS	683 sh	686	684	686	670 sh			668 sh
ν_{48}	646	651	644	651	639			
ν_{48}		638	637	638		633	635	638
ν_{24}	604	603			604			
γ_{21}	569	565	565	565	565	565	567	565
γ_{21}	561	555	556	554 sh	559	548		552
γ_{12}	520	517	517			519		517
ν_{33}	461		458		477	477		478
γ_{22}	438		437	437	454	448		447
$\delta C_\beta C_a C_{Me}$	415	414	413	414	420	418	420	419
$\delta C_\beta C_a S$	405	402	403	402	398	398	396	398
$\delta C_\beta C_c C_d$	384	382	386	382	379	382	378	381
ν_{50}					353			
ν_8	347	348	348	348	349	348	351	348
ν_{51}			323					
	287		303		292			
ν_9	267	266	269	267	258	262	260	261
	245	246	242					
			216				216	

[a] C_a/C_c is the thioether/propionate substituent carbon bound to the pyrrole C_β carbon. $\delta C_\beta C_a C_{Me}$ and $\delta C_\beta C_a S$ are thioether bending. $\delta C_\beta C_c C_d$ is propionate bending. γ is the tetrapyrrole torsional mode.

In the low-frequency region (750−150 cm^{-1}), RR spectra of both cytochromes, in the oxidized and reduced states, have been obtained by Soret excitation. The corresponding frequencies are listed in Table 2. The vibrational assignment proposed for ferrous yeast iso-1-cytochrome *c* (Hu et al., 1993) has been adopted; though one of the axial ligands is different, it was demonstrated (Hu et al., 1993) that no vibrational mode due to these ligands is detectable. As expected, the distinctive features of the low-frequency spectrum of ferrocytochrome *c*, *i.e.* the strong intensity of the depolarized ν_{15} mode, when Soret excited, and the splitting of numerous vibrational modes, are no longer present. The vanishing of one of the components of the doublets gives rise to distinctive vibrational patterns for the two cytochromes, in the same oxidation state, and for the two oxidation states of the same cytochrome. This last point is the only relevant one for our present work. Most noticeable is the very strong increase of the intensity of the C_a-S stretching mode for reduced cyt.c_3; the increase of the intensity of the $C_\beta C_a S$ bending mode, in the case of D.v.H. cyt.c_3, is also worth mentioning.

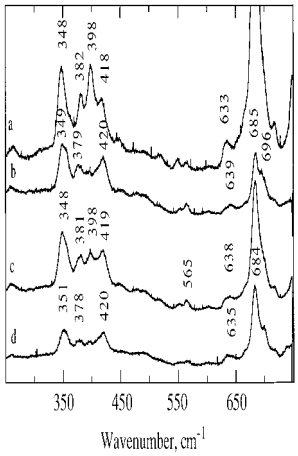

FIGURE 8: Low-frequency RR spectra of D.v.H. cyt.c_3 (excitation, 413.1 nm, 10 mW): (a) $(Fe^{II})_4$; (b) $(Fe^{III})_4$; (c) intermediate, calculated; and (d) intermediate, experimental.

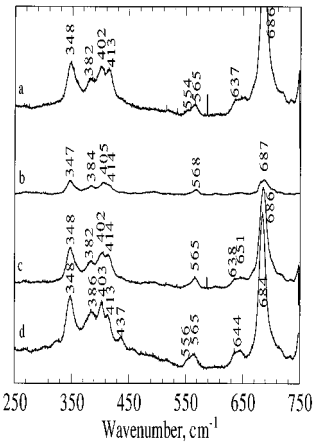

FIGURE 9: Low-frequency RR spectra of D.d.N. cyt.c_3 (excitation, 413.1 nm, 10 mW): (a) $(Fe^{II})_4$; (b) $(Fe^{III})_4$; (c) intermediate, calculated; and (d) intermediate, experimental.

Careful comparison of the experimental and calculated spectra for the intermediate state reveals the following differences.

For D.v.H. cyt.c_3, in the intermediate state $(Fe^{III})_3(Fe^{II})$ (Figure 8), those differences include the occurrence of a shoulder at 699 cm^{-1}, assigned to ν_7; the downshift of the bands ν_{48}, $\delta C_\beta C_a S$, $\delta C_\beta C_c C_d$, centered at 635 (−3), 396 (−2), and 378 (−3) cm^{-1}, respectively, the latter being broadened; and the upshift of the ν_8 band, centered at 351 (+3) cm^{-1}.

Thus, the major changes involve (i) the bending modes of the propionate substituents $\delta C_\beta C_c C_d$, whose frequencies are spread out, and (ii) two planar vibrations of the tetrapyrrole ring, ν_7, the symmetric bending (and, more difficult to ascertain, due to its weak intensity, ν_{48}, the asymmetric bending), and ν_8, which is mainly the FeN stretching. The latter is slightly strengthened.

For D.d.N. cyt.c_3, in the intermediate state $(Fe^{III})_2(Fe^{II})_2$ (Figure 9), the differences include the occurrence of two distinct shoulders at 558 and 439 cm^{-1}, assigned to the torsion modes γ_{21} and γ_{22}, respectively, and the downshift of the maximum of the νC_aS band, localized at 684 cm^{-1} (−2), and the upshift of the $\delta C_\beta C_c C_d$ band, localized at 386 cm^{-1} (+4).

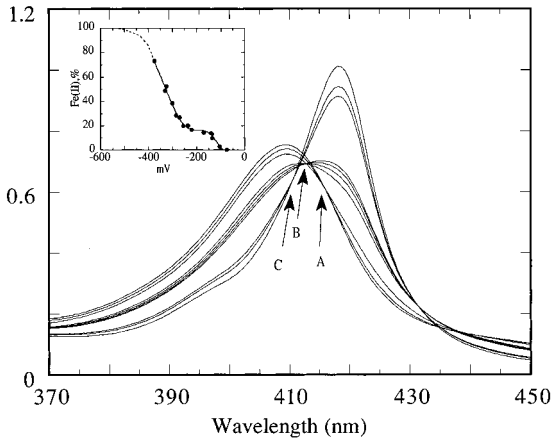

FIGURE 10: Absorption spectra of D.v.H. cyt.c_3 H25M, in the Soret band (Tris-HCl buffer, 50 mM, pH 7.5), at increasingly negative potentials from 0 V $(Fe^{III})_4$ to −420 mV $(Fe^{II})_4$. (Inset) Titration plot.

Thus, the main changes involve (i) the bending modes of the propionate substituents and (ii) two out-of-plane bending modes of the tetrapyrrole ring (γ_{21} and γ_{22}) and the C_a−S stretching mode, between the carbon atom adjacent to the pyrrole and the sulfur atom of the cysteine. These last three vibrations are related to the attachment of the cysteine residue to the tetrapyrrole ring and the resulting puckering of the ring.

In the intermediate state, both cytochromes display bending frequencies of the propionate substituents that deviate from what is expected. Other observed deviations depend on the cytochrome under consideration. In the case of the D.v.H. cyt.c_3, planar vibrations of the tetrapyrrole that could reflect a change in the coupling of the Fe(III) hemes are modified; in the case of the D.d.N. cyt.c_3, the modified vibrations can be related to the heme puckering due to the attachment of the cysteine residue to the tetrapyrrole.

Visible Spectroelectrochemistry of the D.v.H. cyt.c_3 Mutant H25M

The D.v.H. cyt.c_3 mutant H25M, in which histidine 25, the sixth ligand of heme III, is replaced by a methionine, has already been characterized by mass spectrometry and absorption spectroscopy, and its redox potentials have been measured (Dolla et al., 1994). The absorption spectrum of the H25M mutant is almost identical to that of the wild type cytochrome, except for a low-intensity band centered at 695 nm, characteristic of the iron−methionine ligation. One of its redox potentials is definitely higher (−90 mV) than the three others (−285, −305, and −310 mV), in agreement with what is expected from the replacement of a histidine by a methionine (Dolla et al., 1994).

The Soret absorption monitoring of the electron transfer (Figure 10) reveals three distinct isosbestic points located at 416 nm, up to 25% reduction, 412.2 nm for a reduction ratio between 25 and 50%, and 411 nm for reduction ratios higher than 50%. At variance with the properties of the wild type cytochrome, outside the Soret band, all the isosbestic points are doublets; for example, the point at 432.6 nm in the wild type cytochrome is located at 438.1 nm for less than 25% reduction and shifts to 431.4 nm till the end of the reduction. This suggests the following reduction scheme:

$$(Fe^{III})_4 \rightleftharpoons (Fe^{III})_3(Fe^{II}) \rightleftharpoons (Fe^{III})_2(Fe^{II})_2 \rightleftharpoons (Fe^{II})_4$$

The titration plot (Figure 10) presents a plateau, corresponding to the titration of the first heme, with $E_{1/2} = -130$ mV, the three other hemes being reduced at a mean potential of −320 mV, identical to that of the wild type cytochrome.

The differential absorption spectrum $S_x - S_{ox}$, where S_x corresponds to a reduction ratio x of 25%, has been obtained (Figure 11a). The negative band, corresponding to the missing Fe(III), is centered at 406.6 nm, distinctly blue-shifted when compared to that of the wild type cytochrome. This clearly shows that the high-potential hemes are different in both cases.

CD monitoring of the electron transfer has been undertaken. The CD signals of the all-ferric and all-ferrous states are almost identical to those of the wild type cytochrome. On the contrary, the CD signals, observed for reduction ratios between 25 and 50%, are different from those of the wild type cytochrome (Figure 11b); they are composed of a large intense positive band and a narrow medium intensity negative band. Moreover, they cannot be fitted by a linear combination of the $(Fe^{III})_4$ and $(Fe^{II})_4$ signals. As a matter of fact, they offer a strong resemblance to the CD signal of the half-reduced state of D.d.N. cyt.c_3.

DISCUSSION

The analysis of the results of the absorption spectroelectrochemistry experiments has shown that an intermediate is involved in the electron transfer, in the case of both D.v.H. cyt.c_3 and D.d.N. cyt.c_3. The presence of such an intermediate is sensitive neither to pH variations, in the 5.5−9.2 range, nor to ionic strength variations up to 0.5 M. The main difference between both cytochromes is that the intermediate is formed after the introduction of the first electron, in the case of D.v.H. cyt.c_3, and of the second electron, in the case of D.d.N cyt.c_3.

The occurrence of an intermediate has already been shown in the case of D.v.M. cyt.c_3, a cytochrome highly homologous to D.v.H. cyt.c_3 (Tabushi et al., 1983; Yagi, 1984). Our results are in good agreement with those of Yagi, who assigned the Soret spectral abnormality, in the course of the enzymatic reduction of D.v.M. cyt.c_3, to the formation of a $(Fe^{III})_3Fe^{II}$ intermediate. They are compatible with the biphasic kinetics observed for the reduction of D.v.H. cyt.c_3 by sodium dithionite (Capellière-Blandin et al., 1986) and agree even better with the kinetics data obtained for the reduction of D.g. cyt.c_3 [a cytochrome 47.4% homologous to D.v.H. cyt.c_3 (Matias et al., 1993)], showing that the observed fast phase corresponds to the reduction of the highest-potential heme (Catarino et al., 1991).

We have carried out a characterization of this intermediate. Its differential absorption and CD spectra show that its Fe(II) component has electronic properties different from those of the $(Fe^{II})_4$ state; the nonexcitonic character of the Fe(II) component of the CD signal shows that the additional electron is mainly localized on a single heme, which should be heme IV, according to Salgueiro et al. The RR data reveal perturbations of low-frequency vibrations, mostly located at the heme periphery, *i.e.* methine bridges and propionate and cysteine substituents. A small strengthening of the Fe−N bonds is also noticeable, in the case of the D.v.H. cyt.c_3.

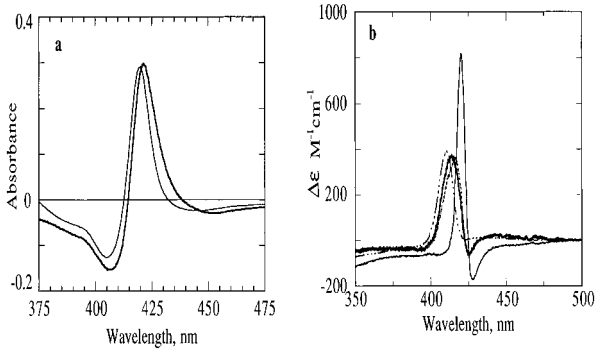

FIGURE 11: (a) Soret differential absorption spectra (spectrum at potential E − spectrum at potential 0, E = potential to achieve 25% reduction) of D.v.H. cyt.c_3 H25M: (dark line) experimental and (light line) calculated. (b) Soret CD spectra of D.v.H. cyt.c_3 H25M: (−···−) $(Fe^{III})_4$, (light line) $(Fe^{II})_4$, (dark line) $(Fe^{III})_3Fe^{II}$, and (- - -) $(Fe^{III})_2(Fe^{II})_2$.

The RR monitoring of the entire electrochemical redox process did not reveal any multiple splittings of the main high-frequency Raman bands, at variance with the results described for the enzymatic reduction of the highly homologous D.v.M. cyt.c_3 (Verma et al., 1988). Vibrational coupling was proposed as the origin of these splittings. Previous attempts to observe such splittings on μ-oxo dimers of iron tetraphenylporphyrin (Adar & Strivastava, 1975 ; Burke et al., 1978) and iron protoporphyrin IX (Hoffman & Bocian, 1984) gave negative results; we did not observe any splitting on D.d.N. cyt.c_3 either, though our CD data (*vide infra*) are in favor of a specific excitonic coupling for the half-reduced state.

In the case of D.d.N. cyt.c_3, a conformational change associated with the uptake of two electrons has been described by UV−visible differential absorption and FTIR spectroelectrochemistry (Schlereth et al., 1993). In good agreement, our results point also to the presence of an intermediate at half-reduction, for this cytochrome. Our CD study reveals an intense typical CD signal in the Soret region, corresponding to a specific coupling of the hemes, at half-reduction. The RR data show that the propionate deformation as well as three other vibrations, involved in the attachment of the cysteine to the pyrrole ring, and the resulting ruffling of the heme are modified.

The above-mentioned results show that, though an intermediate is involved in the electron transfer for both cytochromes, the accompanying structural changes are not alike. In order to get a better understanding of the conformational change, we should consider the following points. (i) The titration plots for both cytochromes are very different; (ii) the plateau in the titration plot of D.d.N. cyt.c_3 corresponds to the reduction of the first high-potential heme, whereas the conformational change occurs after reduction of the second heme.

Therefore, the conformational change is linked neither to a particular distribution of the potentials (one higher and three lower vs four close values) nor to the reduction of the first high-potential heme. If one takes into account the potential order proposed for the two cytochromes, *i.e.* HIV > HI > HII > HIII for D.v.H. cyt.c_3 and HIII > HIV > HI > HII for D.d.N. cyt.c_3, then it comes out clearly that it is the reduction of heme IV that triggers the conformational change. This fits well with the results on the D.v.H. cyt.c_3 H25M mutant; three successive isosbestic points appear in the Soret band in the course of the electron transfer. The first one corresponds to the reduction of heme III, bearing the mutation, and the second could correspond to the reduction of heme IV (first heme reduced for the wild type cytochrome), if the only effect of the mutation is to raise the potential of heme III. Interestingly, at half-reduction, this mutant displays a CD signal much like that of half-reduced D.d.N. cyt.c_3. This CD signal may then be considered as characteristic of a state in which hemes III and IV are reduced while hemes I and II remain oxidized. This way, it gives support to the description of the three-dimensional structure of D.d.N. cyt.c_3 as composed of two two-heme-containing domains (N-terminal domain, hemes I and II; C-terminal domain, hemes III and IV, both bound to the main α helix) (Pierrot et al., 1982; Czjzek et al., 1994) and stresses the specificity of the heme−heme interactions when the C-terminal domain is reduced, while the N-terminal domain remains oxidized.

The position of heme IV in the electron transfer chain is not a determining factor for the conformational change; therefore, the function of heme IV must rely on the specificity of its structural environment. Our results show that the reduction of a heme anchored in one of the helices (heme III) is not followed by a reorganization of the molecule, whereas the reduction of a heme (heme IV) located in a region surrounded by flexible loops triggers a conformational change. Indeed, in these conditions, the effect of the charge variation on the iron, during the electron transfer, could stabilize one of the available conformations of the protein chain.

At this stage, two hypotheses can be formulated.

Reduction of heme IV, the first or second step in the intramolecular electron transfer, induces a conformational change that would modify the potential of the neighboring hemes, initially very close, so as to control the spontaneous sense of the electron transfer.

Heme IV is located in the vicinity of lysine residues that are involved in complex formation with partner proteins, as demonstrated by peptide mapping of the cross-linked complex between D.d.N. cyt.c_3 and D.d.N. ferredoxin I (Dolla et al., 1991). The conformational change linked to its reduction could be a signal that modulates the interaction of cytochrome c_3 with these proteins.

ACKNOWLEDGMENT

The authors are grateful to Dr. A. Dolla for a gift of D.v.H. cyt.c_3 H25M and to Dr. M. Czjzek for helpful comments.

REFERENCES

Adar, F., & Strivastava, T. (1975) *Proc. Natl. Acad. Sci. U.S.A. 72*, 433.
Akutsu, H., Hazzard, J. H., Bartsch, R. G., & Cusanovich, M. A. (1992) *Biochim. Biophys. Acta 1140*, 144−156.
Bianco, P., & Haladjian, J. (1981) *Electrochim. Acta 26*, 1001−1004.
Bruschi, M., Hatchikian, C. E., Golovleva, L. A., & Le Gall, J. (1977) *J. Bacteriol. 120*, 30−38.
Burke, J. M., Kincaid, J. R., & Spiro, T. G. (1978) *J. Am. Chem. Soc. 100*, 6077.
Capellière-Blandin, C., Guerlesquin, F., & Bruschi, M. (1986) *Biochim. Biophys. Acta 848*, 279−293.
Catarino, T., Coletta, M., Le Gall, J., & Xavier, A. V. (1991) *Eur. J. Biochem. 202*, 1107−1113.
Coutinho, I. B., Turner, D. L., LeGall, J., & Xavier, A. V. (1993) *J. Biochem. 294*, 899−908.

Czjzek, M., Payan, F., Guerlesquin, F., Bruschi, M., & Haser, R. (1994) *J. Mol. Biol. 243*, 653−667.
Devereux, R., He, S. H., Orkland, S., Atahl, D. A., Le Gall, J., & Whitman, W. B. (1990) *J. Bacteriol. 172*, 3609−3619.
Dolla, A., Guerlesquin, F., Bruschi, M., Guigliarelli, B., Asso, M., Bertrand, P., & Gayda, J. P. (1989) *Biochim. Biophys. Acta 975*, 395−398.
Dolla, A., Leroy, G., Guerlesquin, F., & Bruschi, M. (1991) *Biochim. Biophys. Acta, 1058*, 171−177.
Dolla, A., Florens, L., Bianco, P., Haladjian, J., Voordouw, G., Forest, E., Wall, J., Guerlesquin, F., & Bruschi, M. (1994) *J. Biol. Chem. 269*, 6340−6346.
Fan, K., Akutsu, H., Kyoguku, Y., & Niki, K. (1990) *Biochemistry 29*, 2257−2263.
Guerlesquin, F., Bruschi, M., & Wüthrich, K. (1985) *Biochim. Biophys. Acta 830*, 296−303.
Guigliarelli, B., Bertrand, P., More, C., Haser, R., & Gayda, J. P. (1990) *J. Mol. Biol. 216*, 161−166.
Hagen, W. R. (1989) *Eur. J. Biochem. 182*, 523−530.
Higuchi, Y., Kusunoki, M., Matsuura, Y., Yasuoka, N., & Kakudo, M. (1984) *J. Mol. Biol. 172*, 109−139.
Hoffman, J. A., & Bocian, D. F. (1984) *J. Phys. Chem. 88*, 1472.
Hu, S., Morris, Y. K., Singh, J. P., Smith, K. M., & Spiro, T. G. (1993) *J. Am. Chem. Soc. 115*, 12446−12458.
Kitagawa, T., Kyogoku, Y., Izuka, T., Ikeda-Saito, M., & Yamanaka, T. (1975) *J. Biochem. 78*, 719−728.
Kitagawa, T., Ozaki, Y., Teraoka, J., Kyogoku, Y., & Yamanaka, T. (1977) *Biochim. Biophys. Acta 494*, 100−114.
Le Gall, J., & Fauque, G. (1988) in *Biology of Anaerobic Microorganisms* (Zehnder, A. J. B., Ed.) pp 587−639, John Wiley, New York.
Le Gall, J., Moura, J., & Dragoni, N. (1965) *Biochim. Biophys. Acta 99*, 385−387.
Lexa, D., Savéant, J.-M., & Zickler, J. (1977) *J. Am. Chem. Soc. 99*, 2786−2790.
Matias, P. M., Frazao, C., Morais, J., Coll, M., & Carrondo, M. A. (1993) *J. Mol. Biol. 234*, 680−699.
Morais, J., Nuno Palma, P., Frazao, C., Caldeira, J., Le Gall, J., Moura, I., Moura, J. J. G., & Carrondo, M. A. (1995) *Biochemistry 34*, 12830−12841.
Moreno, C., Campos, A., Teixeira, M., Le Gall, J., Montenegro, M. I., Moura, I., van Dijk, C., & Moura, J. G. J. (1991) *Eur. J. Biochem. 202*, 385−393.
Morimoto, Y., Tani, T., Okumura, H., Higuchi, Y., & Yasuoka, N. (1991) *J. Biochem 110*, 532−540.
Park, J.-S., Kano, K., Niki, K., & Akutsu, H. (1991) *FEBS Lett. 285*, 149−151.
Pierrot, M., Haser, R., Frey, M., Payan, F., & Astier, J.-P. (1982) *J. Biol. Chem. 257*, 14341−14348.
Postgate, J. R. (1984) in *The Sulfate-Reducing Bacteria*, 2nd ed., Cambridge University Press, Cambridge.
Salgueiro, C. A., Turner, D. L., Santos, H., Le Gall, J., & Xavier, A. V. (1992) *FEBS Lett. 314*, 155−158.
Santos, H., Moura, J. J. G., Moura, I., Le Gall, J., & Xavier, A. V. (1984) *Eur. J. Biochem. 141*, 283−296.
Schlereth, D. D., Fernandez, V. M., & Mäntele, W. (1993) *Biochemistry 32*, 9199−9208.
Sokol, W. F., Evans, D. H., Niki, K., & Yagi, T. (1980) *J. Electroanal. Chem. 108*, 107−115.
Tabushi, I., Nishiya, T., Yagi, T., & Inoguchi, H. (1983) *J. Biochem. 94*, 1375−1385.
Verma, A. L., Kimura, A., Nakamura, A.,Yagi T., Inoguchi, H., & Kitagawa, T. (1988) *J. Am. Chem. Soc. 110*, 6617−6623.
Yagi, T. (1984) *Biochim. Biophys. Acta 767*, 288−294.

BI9608424